School of Natural Sciences and Mathematics

Tunable Organic PV Parallel Tandem with Ionic Gating—Supplement

UT Dallas Author(s):

Alexander B. Cook
Jonathan D. Yuen
Anvar Zakhidov

Citation:

Saranin, Danila, Artur Ishteev, Alexander B. Cook, Jonathan D. Yuen, et al. 2017. "Tunable organic PV parallel tandem with ionic gating." Journal of Renewable and Sustainable Energy 9(2), doi:10.1063/1.4979900

Tunable Organic PV Parallel Tandem with Ionic Gating

Danila Saranin[1,3], Artur Ishteev[1], Alexander B. Cook[2], Jonathan D. Yuen[2], Denis Kuznetsov[1], Marina Orlova[3], Sergey Didenko[3] and Anvar Zakhidov[1,2]

[1]Energy Efficiency Center, National University of Science and Technology, MISiS, Moscow, Russia, 119049

[2]Physics Department and the NanoTech Institute, The University of Texas at Dallas, Richardson, USA, 75080

[3]Department of semiconductor electronics and physics of semiconductor devices, National University of Science and Technology, MISiS, Moscow, Russia, 119049

Supplementary Information.

Experimental details

Device Fabrication:

Firstly ITO pixelated substrates (LUMTEC, 15 Ohm/sq) were cleaned in acetone, toluene, IPA (all ME grade) ultrasonic bath with 15 minutes for each step. Then substrates were carefully dried under nitrogen flow, after this substrates were activated by UV treatment during 15 minutes. Device layers were deposited by spin coating in the next sequence:

PEDOT:PSS – 3000 RPM, 60 s, (30 nm thickness), annealing at 150 °C, during 15 min, 5 min cooling.

For PTB7 sub- cell

PTB7:PCBM– 1000 RPM, 60 s, (90 nm thickness), Drying in Antichamber during 30 min, Methanol wash at 2500 RPM (40 s).

Solution details:

Solution was prepared in CB with 1:1,5 weight ratio of PTB7 (Sigma Aldrich) to PCBM (DYE SOURCE) and 3 % DIO addition , 25 mg/ml overall concentration, shaking during 3 hours.

For P3HT sub-cell

P3HT:PCBM – 1000 RPM, 60 s, (200 nm thickness), Annealing at 140 °C for 15 minutes

Solution details:

Solution was prepared in CB with 1:1 weight ratio of P3HT (Rieke metals) to PCBM (DYE SOURCE), 40 mg/ml overall concentration, heating at 50 °C and stirring overnight.

Cathode deposition

CNT electrodes were deposited by lamination of 1 layers for working electrode (cathode) and 5 layers for counter electrode (in air), then they were densified with by HFE. Device pixel formed square of 0,084 cm^2.

After this a small drop 20 µl of ionic liquid was put on PTB7 sub- cell, and gently pressed by P3HT sub- cell from the top to place cells pixels directly under each other.

Finally, silver contacts were painted for SMU connection by clips.

Device characterization:

Measurement was done under standard conditions 1.5 AM, 100 mW/cm^2 with calibrated Thermo Oriel ABA solar simulator and two Keithleys 2400 SMU (for IV characterization and EDLC charging).

1. Charging current dynamics at different V_{gate} and confirmation of PCBM n-doping at higher V_{gate}.

For independent second confirmation of suggested n-doping process of polymer itself at higher gate voltages $V_g > V_{threshold}$, i.e. to prove the charge injection to PCBM LUMO level (and/or to donor polymer HOMO level), the charging currents Ich of gate MWCNT electrode (on top of PCBM layer) and counter-electrode were measured at different V_{gate}. In this method, we observed the time dependent process of double layer charge formation on WMCNT and dynamics of injection processes (first to MWCNT and further to PCBM LUMO level). This type of characterization was performed by measuring the time dependence of charging current between gate MWCNT electrodes and counter-electrode MWCNT at static potential regime at different V_{gate} values (from 0 to 2.25 V with 0.25 V step).

Charging currents were measured for P3HT and PTB7 sub-cells separately. Time dependence of current between MWCNT electrodes presented on figures 20,21, which corresponds to V_{gate} less than threshold 1.5 V (fig.18(a), 19(a) and at Vgate larger than threshold 1.5 V (fig.18(b),19(b)).

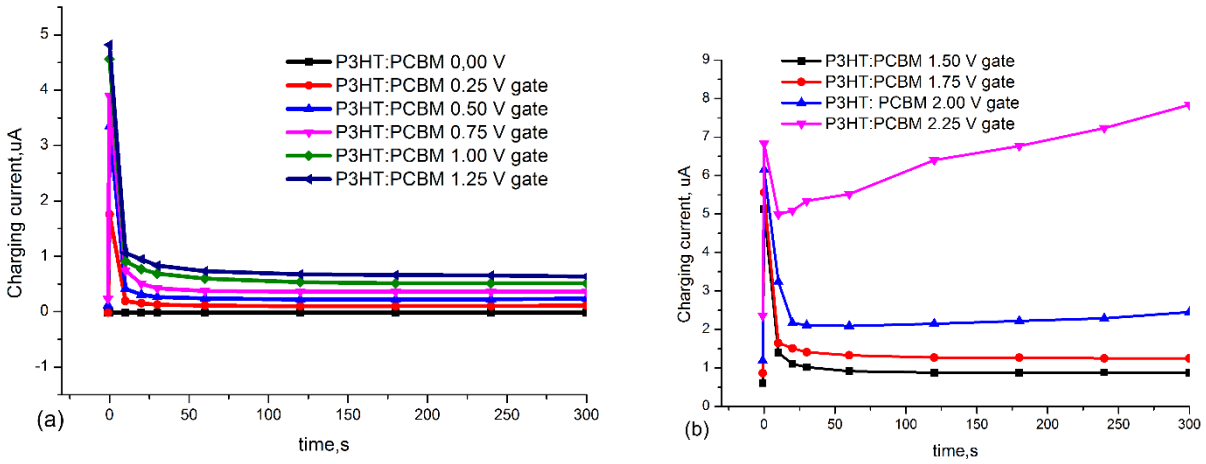

FIG. 18. Time dependence of charging current between MWCNT electrodes in P3HT sub-cell at Vgate<1.5 V (a) and Vgate ≥ 1.5 V

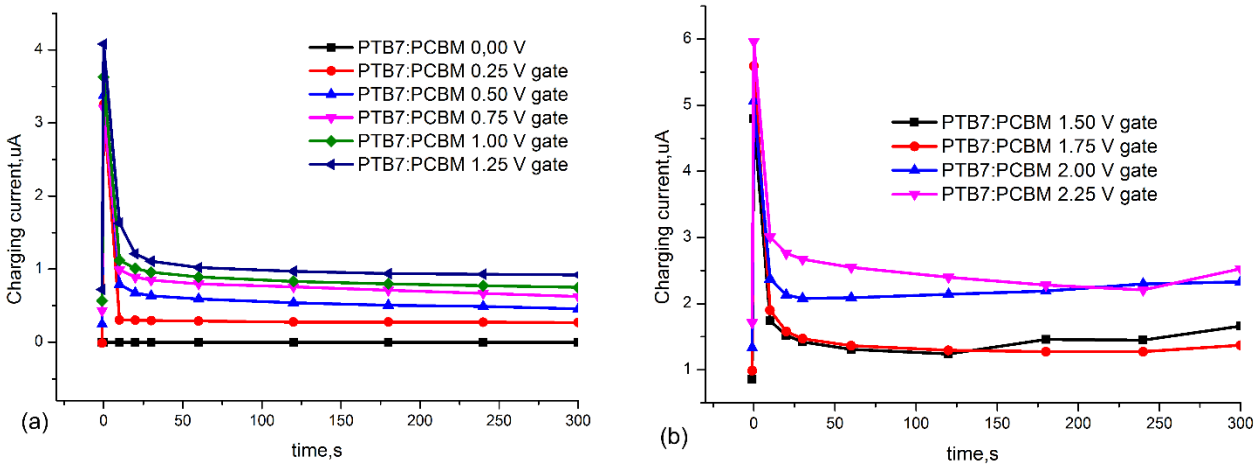

FIG.19. Time dependence of charging current between MWCNT electrodes in PTB7 sub-cell at Vgate<1.5 V (a) and Vgate ≥ 1.5 V

Another effect of doping in sub-cells was observed visually. At high Vgate voltages, 1.75 V for PTB7 sub cell and 2.25 V for P3HT sub-cell, we found that color of sub cells' bulk heterojunctions has been changed during gating process. Real photos of separately fabricated sub-cells are presented on Figure 20 (a)(b).

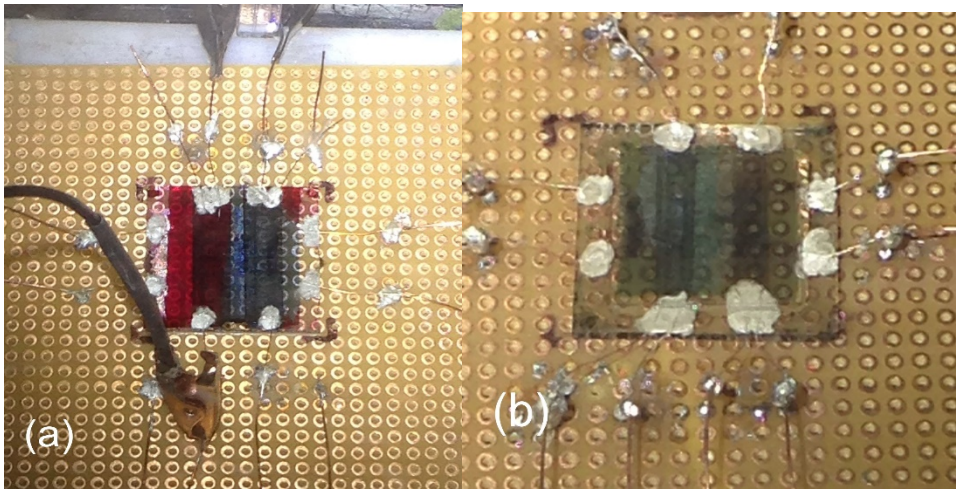

FIG.20. Real photos of separately fabricated sub-cells during ionic gating of P3HT sub-cell (a) and PTB7 sub-cell (b)

This results of charging current time dependence and its qualitative changes with increasing Vgate show clear dynamics of I_{ch} slow growth with time due to secondary electron injection from CNT to PCBM and further, which we use as independent confirmation of n-doping process been extended from MWCNT electrode to a second network of layers in OPV. This second network slow charging confirms our PCBM n-doping hypothesis. We notice that at V_{gate} below 1.5 V (graphs 20a and 21a for each sub- cells) charging current have a usual sharp peak, followed by fast decay and

saturation, which corresponds to first moment of applied V_{gate}. This peak and its later drop to saturation shows fast dynamics of EDLC formation at MWCNT interfaces with e^- injection into CNT with charging current (for charge balancing of plus ions on CNT, that penetrated into CNT from ionic liquid), because its value growth proportionally to V_{gate}. The charging peaks with fast decay has been described earlier in [35, 36, 40], but only at low Vgate. We here observe a new behavior at $V_{gate} > V_{thr}$, namely a secondary slow growth of charging current after the initial fast drop of I_{ch}. which can be interpreted as complex dynamics of charging of two capacitors, connected in parallel. First capacitor between two MWCNT electrodes, and the second capacitor formed of PCBM molecular network and MWCNT counter-electrode. First capacitor is actually a MWCNT supercapacitor with huge capacitance due to high porosity and it is charged very fast due to fast electron injection to CNTs and fast ions insertion between bundles of CNT tubes with formation of EDLC. When Fermi level in CNT is raised to the level of LUMO in PCBM the electrons are injected from CNT to PCBM, slowly charging the PCBM-CNT capacitor. This process is slow due to much slower diffusion of plus ions in BHJ layer, i.e. between chains of polymer donor, before they reach PCBM This independently confirms our hypothesis of electron injection from MWCNTs to chains of PCBM, before they start doping chains of PTB7 at even higher gating. This process of PCBM n-doping is observed as improved I-V curves of OPV, due to better interface resistance between CNT and n-doped PCBM. This I-V improvement happens exactly at same V_{gate}, when injection of e^- to PCBM LUMO is observed in charging current.

Similarly for second sub-cell with BHJ of P3HT:PCBM the gating behavior is qualitatively same: At $V_{gate} \geq 1{,}5$ V we observed similar initial behavior of charging current: a fast peak, followed by fast decay, but after the decay, the charging I_{ch} curve changes its behavior from saturation tail to a slow growth at V_{gate} above 1.5-1.75 V and further to significant growth of Ich current growth with time at V_{gate} above 2.0-2.25 V. After 300 seconds of ionic gating processes charging current got it saturation after its growth. P3HT sub-cell shows its charging current growth at higher V_{gate} (2.0 V) in comparison to PTB7 cell (1.75 V) because of higher levels of HOMO/LUMO. So, this effect of charging current gain during ionic gating at high Vgate can show e^- injection to donor LUMO. Moreover it fits to output JV performance changes and finally we obtained BHJ color changes (P3HT BHJ to blue and PTB7 BHJ to yellow). The effect of optical properties of polymers (under MWCT electrode) tuning via ionic gating will be presented in separate paper in more details.

Reproducibility of gating results and errors

The process of ionically gated OPV tandem fabrication was reproduced three times on separately fabricated sub-cells, error bars present figure 9-12 in paper text. On the other hand output performance during ionic gating process of tandem device can be repeated at different gate voltages after discharging process (changing of V gate value to 0 V). During discharging process current between MWCNT electrodes drops to initial value at zero gate voltage (~ tens of nA) and then output performance of device can be repeated again (presented on FIG.21). Initial charging current between MWCNT electrodes at zero gate voltage caused by small electric field formed by low Voc of sub-cells.

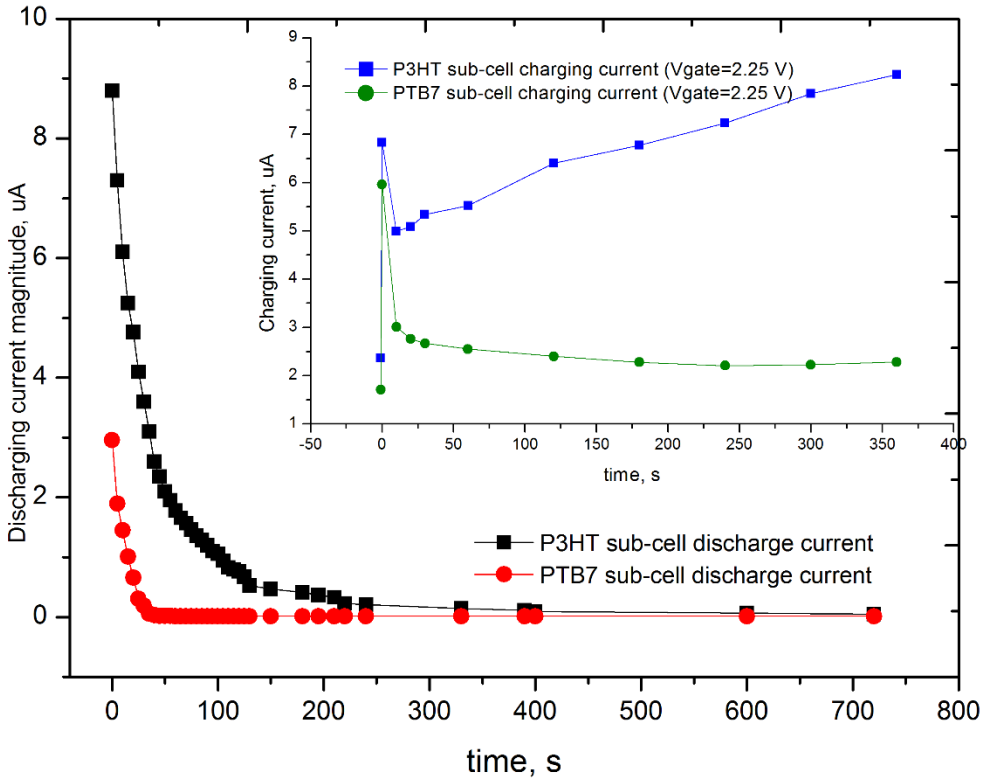

FIG.21. Inset charging and discharging graphs for P3HT and PTB7 sub-cell respectively after same high V_{gate} applied.

It's clear that discharging rate of PTB7 sub cell much more higher that rate of P3HT sub-cell, this means last one has higher capacitance of surface charged layer with CNT electrode. Indeed P3HT based sub-cell has higher charging current secondary raise at same V_{gate}=2.25 V (shown at inset) as compared to PTB7 sub-cell. Therefore the discharged of higher charged P3HT sub-cell goes at

slower rate. Another possible reason is that plus ions movement from BHJ with P3HT is by much slower diffusion process as compared to faster movement of ions from more regular PTB7 chains at same initial high charging V_{gate}.

Tab 3. Top ionically gated P3HTcell (in tandem measurements) output parameters

Ugate, V	Uoc (V)	Jsc (mA/cm2)	FF	Efficiency (%)	Rs, Ohm*cm2	Rsh, Ohm*cm2
0	0,004961	0,419868	0,254	5,29E-04	-	-
0,5	0.014	0.176	0.33	0.00087	-	-
0.75	0.015	0.913	0.328	0.0045	-	-
1.0	0.095	1.55	0.240	0.0356	28.	-
1.25	0.205	2.19	0.243	0.11	24.02	3180.00
1.5	0.367	2.684	0.254	0.249	25.55	4005.44
1.75	0.396	3.423	0.295	0.400	39.17	4116.50
2.0	0.477	6.409	0.321	0.982	23.42	5154.36
2.25	0.427	4.235	0.421	0.763	15.78	5288.58

2. Supplementary Data and Figures for P3HT based sub-cell

Accordingly to paper links here presented Supplement about P3HT sub-cell gating process.

The Figures showing energy bands evolution during the ionic gating of a second sub-cell (P3HT/PCBM/CNT PV cell) and the schematics of ions penetration into the CNT network and the depth of BHJ are shown below at Figs. 22-25. Basically quite similar to processes in the first sub-cell, described in main text.

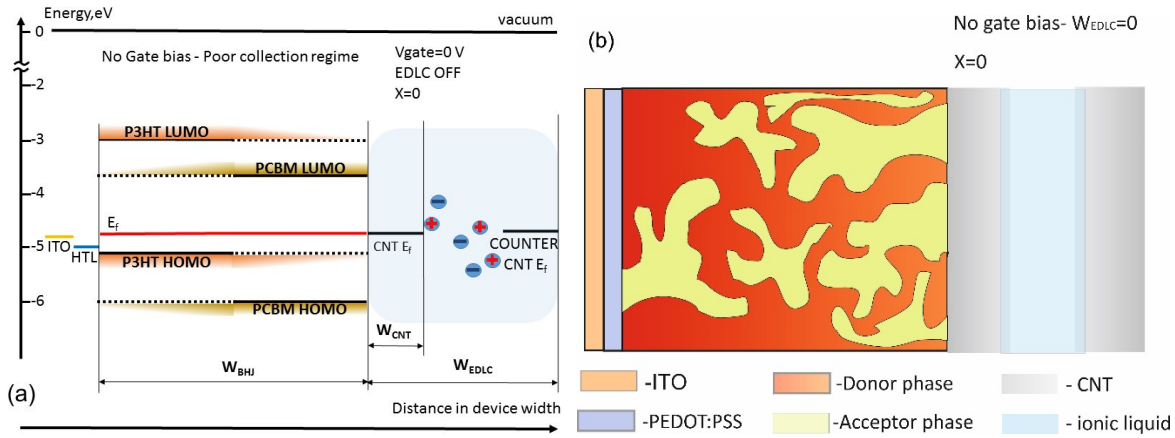

FIG. 22. (a) Band Diagram of front- sub cell at zero Vgate with sketch schematics of EDLC and ion Introduction in device. (b) Sketch schematics of front sub- cell BHJ and CNT interface modification.

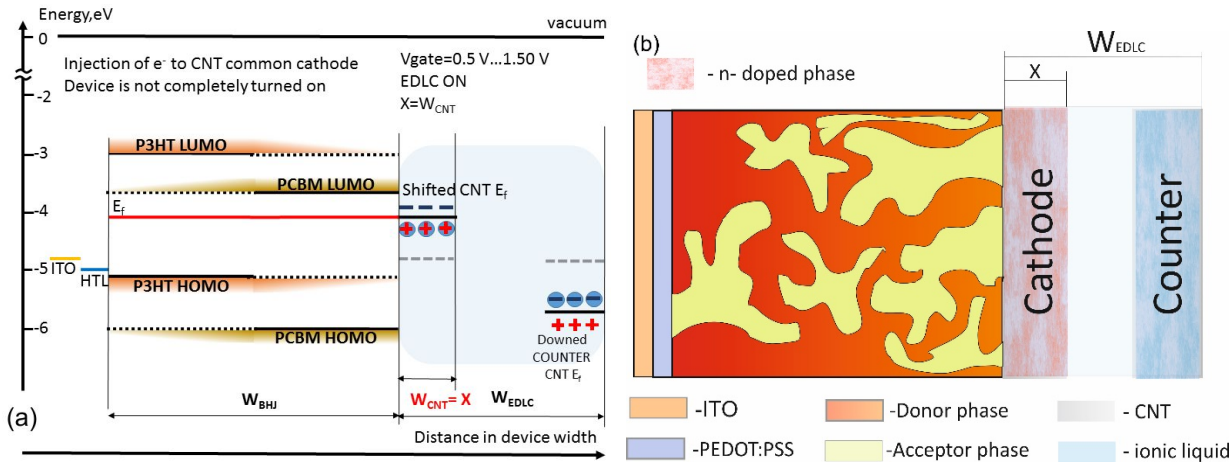

FIG. 23. (a) Band Diagram of front- sub cell at CNT e^- injection process at 0,5…1,50 Vgate with sketch schematics of EDLC and ion introduction in device, when it's not turned on yet.(b) Sketch schematics of front sub- cell BHJ and CNT interface modification.

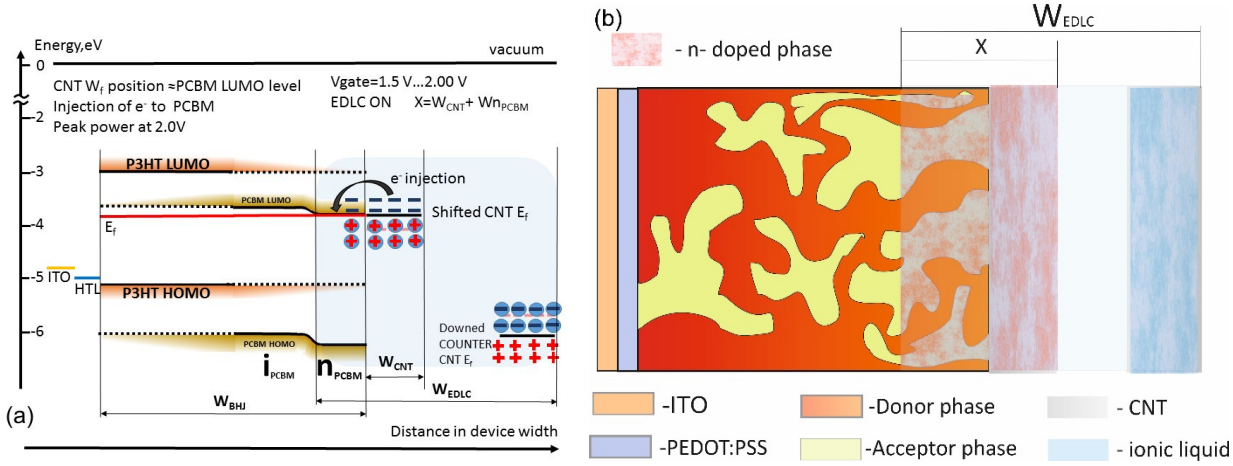

FIG. 24. (a) Band Diagram of front- sub cell at e- injection process to PCBM LUMO level at 1,50-2,0 Vgate with sketch schematics of EDLC and ion introduction in device. (b) Sketch schematics of front sub- cell BHJ and CNT interface modification.

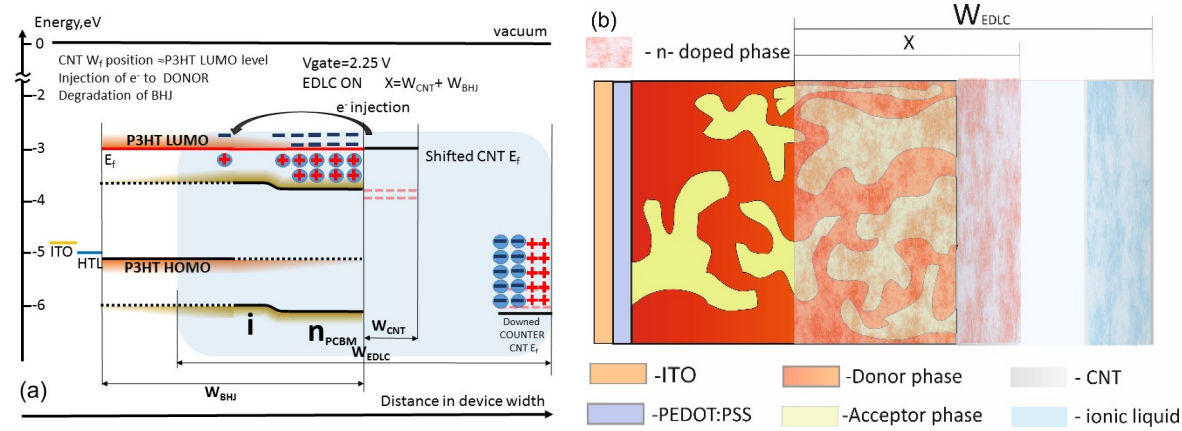

FIG. 25. (a) Band Diagram of front- sub cell at e- injection process to P3HT donor LUMO level at 2,25 Vgate with sketch schematics of EDLC and ion introduction in device. (b) Sketch schematics of back sub- cell BHJ and CNT interface modification.